Spin Density Distribution in a Nitroxide Biradical Containing Acetylene Groups in the Bridge: DFT Calculations and EPR Investigation

A. I. Kokorin[1] · R. B. Zaripov[2] · O. I. Gromov[1,3] · T. Kálai[4] · É. Lamperth[4] · K. Hideg[4]

Received:

Abstract A specially synthesized nitroxide biradical R_6–^{13}C≡C–*p*-C_6H_4–C≡^{13}C–R_6, **B3**, where R_6 = 1-oxyl-2,2,6,6-tetramethyl-3,4-ene- nitroxide ring, have been studied by electron paramagnetic resonance (EPR) spectroscopy, and electron-nuclear double resonance (ENDOR). Spin density distribution and hyperfine splitting (hfs) constant on ^{13}C atoms calculations for biradical **B3** were carried out using B3LYP and PBE0 functionals and several different basis sets including N07 family and were compared with the experimental value of the hfs constant on ^{13}C atoms, measured from ENDOR spectra of **B3**. The mechanism of the intramolecular electron spin exchange in **B3** biradical is discussed.

Key words: EPR spectroscopy, nitroxide biradical, spin density distribution, X-ray structure, DFT calculations

---

A. I. Kokorin (✉)
e-mail: alex-kokorin@yandex.ru

[1] N. N. Semenov Institute of Chemical Physics, Russian Academy of Sciences, Moscow, Russian Federation

[2] Zavoisky Kazan Physical-Technical Institute, Russian Academy of Sciences, Kazan, Russian Federation

[3] Chemistry Department, M. V. Lomonosov Moscow State University, Moscow, Russian Federation

[4] Institute of Organic and Medical Chemistry, University of Pécs, PO Box 99, Pécs 7602, Hungary

1 Introduction

Scientists all over the world have been intrigued by the chemistry of stable free radicals since their discovery in 1900 [1]. Stable radicals of different types are presently uzed in a variety of fields [2] including spin labeling [3-12], the construction of organic magnetic materials [13], MRI contrast agents [14], redox-active components of organic radical batteries [15], co-oxidants [16] and tools for controlled radical polymerization [17]. Some biradicals were found to be promissing polarizing agents for dynamic nuclear polarization [18, 19]. Nevertheless, in many cases, biradical or poliradical structure and features, their magnetic properties are still the subject of investigation [20, 21].

Among numerous nitroxide biradicals, those containing acetylene groups in the bridge connecting two nitroxide rings present an interesting specific group [22-31]. In these biradicals, which are structurally rigid enough, spin exchange coupling between the unpaired electrons is realized by the indirect mechanism via the bridge of atoms and bonds connecting two paramagnetic nitroxide rings [27, 30-32]. The intramolecular dynamics and temperature behaviour in such biradicals dissolved in various molecular and ionic liquid solvents is is usually described well with a two-conformational model [32, 33]. In such biradicals, the intramolecular spin exchange coupling occurs by the indirect mechanism through the bridge of atoms and bonds.

It has been recently shown that such polyacetylene biradicals as R_6–C≡C–R_6 (**B1**), R_6–C≡C–C≡C–R_6 (**B2**), R_6–C≡C–*p*-C_6H_4–C≡C–R_6 (**B3**), and R_6–C≡C–*p*-C_6H_4–C≡C–C≡C–R_6 (**B4**), where R_6 is 1-oxyl-2,2,6,6-tetramethylpiperidine-3,4-ene- nitroxide ring, [30, 31], that nitroxide biradicals with acetylene groups in the bridge are not “rigid” but “flexible”, and biradical **B2** due to fast rotations around its molecular axis even at low temperatures demonstrates average values of the exchange integral $|J|$. Biradical **B3** is characterized by a higher rotation barrier in vacuum and is therefore more rigid. It was concluded from EPR data that both biradicals exist in at least two different conformers with a slight influence of temperature on the $|J/a|$ value. It decreases at high temperature, when faster rotation averages the configurations more effectively [30]. A short nitroxide biradical, **B1**, has been investigated by EPR spectroscopy supplemented with a single-crystal X-ray analysis and DFT calculations [31]. Structural and EPR data were complemented with quantum chemical calculations, and conformational transitions in biradical **B1** were also in a good agreement with quantum chemical computation. Nevertheless, understanding that in such chemically rigid polyacetylene nitroxide biradicals intramolecular spin exchange can be realized only by the indirect mechanism, we

could not measure the spin density distribution on atoms forming the bridge in biradicals, and to describe quantitatively spin delocalization and its influence on the $|J|$ value.

In this work, we present our results on studying the spin density delocalyzation and the mechanism of the intramolecular spin exchange in the nitroxide biradical R_6–^{13}C≡C–*p*-C_6H_4–C≡^{13}C–R_6, **B3**, in which two carbon atons are substituted by ^{13}C isotopes (I = 1/2). Spin coupling in **B3** can be realized only via the bridge of atoms and bonds connecting two 1-oxyl-2,2,6,6-tetramethyl-3,4-ene- nitroxide rings, and it was investigated using EPR, ENDOR spectroscopy as well as quantum chemical calculations.

2 Experimental

2.1 *Synthesis of **B3** biradical*

Methyl-^{13}C-triphenylphosphonium iodide in anhydrous THF suspemsion was treated with butyl lithium solution. To this brown-coloured solution was added the terephthalaldehyde (**1**) and after work-up we got the 1,4-divinylbenzene, of which bromination with 4.4 equiv. Br_2 in $CHCl_3$ gave the tetrabromo product. Elimination with 6 equiv. KO*t*-Bu in THF generated the isotopically labelled 1,4-diethynyl benzene (**2**). The Sonogashira coupling with 4-iodo-2,2,6,6-tetramethyl-1,2,5,6-tetrahydropyridin-1-yloxyl radical [36] in Et_3N and in the presence of CuI and $Pd(PPh_3)_2Cl_2$ biradical (**3**) was generated. According to our experience this synthetic methodology resulted no Glaser-coupled product formation (while paramagnetic acetylenes reaction with 1,4-diiodobenzene generated two types of biradicals).

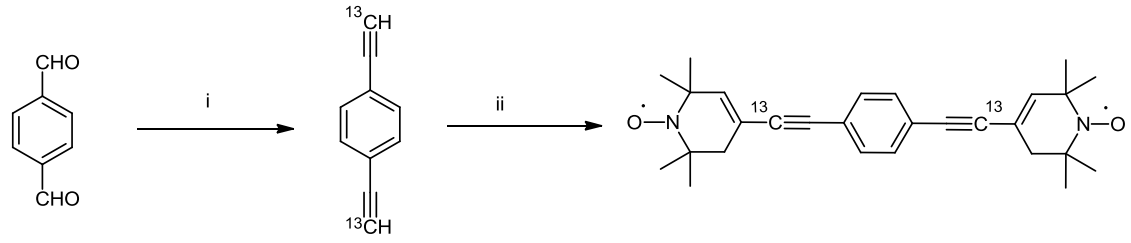

Fig. 1 Scheme of the synthesis of biradical **B3**

Reagents and conditions were: (i) $^{13}CH_3P(Ph)_3I$ (2.18 eq.), BuLi (2.18 eq.), THF, 2h, 0°C, then -78°C, terephthalaldehyde (1.0 eq.) 15 min, rt, 3h, 83% then $CHCl_3$, Br_2 (2.2 eq.), rt, 12h, then KO*t*-Bu (6.0 eq.), THF, reflux, 3h, 60%. (ii) 4-iodo-2,2,6,6-tetramethyl-1,2,5,6-tetrahydropyridin-1-yloxyl radical (2.1 eq.), Et_3N, CuI (0.1 eq.), $Pd(PPh_3)_2Cl_2$ (0.06 eq.), 50°C, 20 h, 25%. Here rt denotes room temperature.

Melting points were determined with a Boetius micro melting point apparatus and are uncorrected. Elemental analyses (C, H, N) were performed on Fisons EA 1110 CHNS elemental analyzer. Mass spectra were recorded on a Thermoquest Automass Multi. ^{1}H NMR and ^{13}C NMR spectra were recorded with Bruker Avance 3 Ascend 500 spectrometer. Chemical shifts are referenced to Me_4Si. The paramagnetic compound was reduced with 5 equiv. pentafluorophenyhydrazine/radical. Measurements were run at 298K probe temperature in $CDCl_3$ or CD_3OD solution. Flash column chromatography was performed on Merck Kieselgel 60 (0.040-0.063 mm). Qualitative TLC was carried out on commercially available plates (20 x 20 x 0.02 cm) coated with Merck Kieselgel GF254. It is essential that anhydr. THF can be used only, Et_3N was distilled from CaH_2 prior to use. Terephthalaldehyde and methyl-^{13}C-triphenylphosphonium iodide and butyl lithium were purchased from Aldrich. 4-Iodo-2,2,6,6-tetramethyl-5,6-dihydropyridin-1-yloxyl radical [36] was prepared according to published procedures, other reagents were purchased from Aldrich or Alfa Aesar.

1,4-Diethynylbenzene (**2**): Methyl-^{13}C-triphenylphosphonium iodide (4.86 g, 12 mmol) was suspended in dry THF (50 ml), cooled to 0°C and *n*-BuLi (4.8 ml, 12.0 mmol, 2.5 mol/l solution in hexane) was added. It was stirred for 2 h at the same temperature, then cooled to -78 °C and the terephthalaldehyde (737 mg, 5.5 mmol) as solution in anhydrous THF was added dropwise. After 15 min of stirring at -78°C, the mixture was warmed to room temperature and stirred for another 3 h. After stopping the reaction with water (50 ml), it was extracted with Et_2O (3 x 20 ml) and the combined organic phases were dried over $MgSO_4$, the pure olefin was obtained by column chromatography to give 1,4-divinylbenzene (600 mg, 83%). The 1,4-divinylbenzene was dissolved in $CHCl_3$ (20 ml), to this solution Br_2 (1.60 g, 10.0 mmol) was added and the mixture was allowed to stay overnight. The solvent and bromine was evaporated off *in vacuo*, the residue was dissolved in THF (30 ml), then KO*t*-Bu (27.6 mmol, 3.10 g) was added in one portion and the mixture was stirred and refluxed for 3 h. After cooling the solvent was evaporated off, the residue was partitioned between Et_2O (30 ml) and 5% aq. H_2SO_4 (10 ml). The organic phase was separated, dried ($MgSO_4$), filtered and evaporated and the residue was purified by flash column chromatography with (hexane/Et_2O, 100:1) to give a brownish-white solid (350 mg, 60 %), mp 93-94°C, R_f 0,37 (hexane), MS (70eV): *m/z* = 128 (M^+, 100), 101 (6) 76 (33). Anal calcd for $C_8{}^{13}C_2H_6$: C, 95.28; H, 4.72, found C, 95.20; H 4.59.

4,4'-(1,4-Phenylenebis(ethyne-2,1-diyl))bis(2,2,6,6-tetramethyl-1,2,5,6-tetrahydropyridin-1-yloxyl) biradical **B3**.

To a degassed solution of 4-iodo-2,2,6,6-tetramethyl-1,2,5,6-tetrahydropyridin-1-yloxyl radical (1.40 g, 5.0 mmol) in anhydrous Et_3N (10 ml), CuI (47 mg, 0.25 mmol) and $PdCl_2(PPh_3)_2$ (112 mg, 0.16 mmol) was added and the mixture was stirred for 15 min, followed by the addition

of ^{13}C containing 1,4-diethynylbenzene (300 mg, 2.34 mmol) and was stirred for 20 h at 50°C under Ar, in a sealed tube. The reaction mixture was diluted with $CHCl_3$ (10 ml), filtered through celite and the solvent was evaporated. The residue was partitioned between $CHCl_3$ (30 ml) and aq. sat. NaCl solution (10 ml), the organic phase was separated, washed with 10 % aq. $Na_2S_2O_3$ (10 ml), water (10 ml), dried ($MgSO_4$) and to this mixture activated MnO_2 (172 mg, 2.0 mmol) was added and the mixture was set aside for overnight. Next the mixture was filtered, evaporated and purified by flash column chromatography (hexane/$CHCl_3$) to give the title compound (254 mg, 25 %) as a deep-yellow solid, mp 233-235°C, R_f : 0.66 (hexane/EtOAc). MS (70eV): *m/z* = 432 (M^+, 42), 402 (29), 372(18), 357 (16), 257 (22), 42 (100). Anal calcd for $C_{26}{}^{13}C_2H_{34}N_2O_2$: C, 78.20; H, 7.92; N, 6.48 found C, 78.15; H, 7.80; N 6.42.

2.2 *EPR measurements*

Toluene was selected as a solvent and was carefully purified according to literature procedure [37]. Solutions were prepared, bubbled with nitrogen for 20-25 min. 0.5 ml of a solution was taken into a thin capillary and degassed by frieze-pump circle to remove oxygen, and sealed off under vacuum. Radical concentrations were sufficiently low ($\leq 4\times10^{-4}$ mol l^{-1}) to eliminate intermolecular exchange broadening of EPR lines [38].

EPR spectra were recorded at X-band on a Bruker EMX-8 spectrometer with a modulation frequency of 100 kHz. Temperatures were controlled with accuracy ±0.5°C at temperatures between −20 and 75°C by means of a JEOL JNM-VT-30 temperature control system. EPR parameters: the hyperfine splitting, hfs, constant on nitrogen ^{14}N atom, *a*, and a value of the exchange integral |*J*/*a*|, which is sensitive to any changes of the spin density distribution of the unpaired electron in the system. The exchange integral values |*J*/*a*| were calculated in accordance with [32, 39]. EPR spectra of biradicals were simulated with the computer program package created by Dr. A. A. Shubin (Boreskov Institute of Catalysis, Siberian Branch, Russian Academy of Sciences) and described in details in Ref. [39]. For our calculations, we used spin-Hamiltonian parameters of similar nitroxide radicals collected in [40].

In liquid solutions with rather low viscosity, the spin Hamiltonian $\hat{H}$ comprises the isotropic hyperfine, the Zeeman interactions and the exchange coupling. In the case when both radical fragments are identical and each carries only one nucleus with a nonzero nuclear spin *I* the following equation is valid [34, 35]:

$$\hat{H} = g\beta_e H_0 (S_z^{(1)} + S_z^{(2)}) + a(S_z^{(1)} I_z^{(1)} + S_z^{(2)} I_z^{(2)}) + J\boldsymbol{S}^{(1)}\boldsymbol{S}^{(2)} \qquad (1)$$

The spin Hamiltonian is here written in frequency units; superscripts 1 and 2 denote different radical fragments; $\boldsymbol{S}^{(k)}$ are electron spin operators; $S_z^{(k)}$ and $I_z^{(m)}$ are projections of the electron

and nuclear spins to the Z-axis, respectively; g is the isotropic g-factor of the radical fragments; β_e is the Bohr magneton; H_0 is the external magnetic field; $a \approx 3 \cdot 10^8$ rad/s denotes the ^{14}N isotropic hyperfine splitting (hfs) constant, and J is the exchange integral. In low-viscous solvents, the tensor of the dipole-dipole coupling is averaged to zero by fast rotation of the biradical molecule [32, 33]. For any individual conformation, the one value of $|J|$ should correctly describe the position and integral intensities of all lines in the EPR spectrum. Values of $|J|$ are usually measured in units of the hfs constant a, i.e. as $|J/a|$, with an accuracy of ±2-3%.

For the two-confformational model [32, 34, 35], the Arrhenius plot of $|J/a|$ should be linear for any biradical, and this allow determining the differences in enthalpies, ΔH, and entropies, ΔS, of these two conformations:

$$\ln|J/a| = \Delta S/R - \Delta H/RT\,, \qquad (2)$$

The experimental observation of such plot confirms the validity of the two-conformational model for a biradical.

2.3 *ENDOR measurements*

For measuring hyperfine splitting (hfs) constants of the interaction between the unpaired electron and ^{13}C nucleus, the ENDOR method suggested by W.B. Mims has been used [41]. In this method, three microwave pulses are used, which form the signal of the stimulated echo. Between the second and the third pulses, the radio-frequency pulse (rf pulse). The signal of the stimulated echo is recorded as a function of the rf pulse.

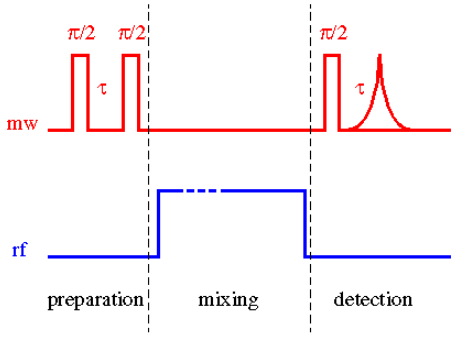

Fig. 2 The scheme of the pulsed ENDOR experiment

Measurements were carried out by using a pulsed EPR spectrometer Elexsys E580 at X-band (10 GHz). A spectrometer is equipped with a standard commercial resonator EN 4118X-MD4W1, which was placed into cryostat CF935. Temperature control was carried out by the ITC503 unit. All measurements were done at 80 K. Two biradicals, **B3** and its analogue **B3a** with a usual

isotope ^{12}C, were investigated. (I = 0). Both biradicals were dissolved in toluene at ~1 mmol/l concentration and degassed by pumping. ENDOR study was performed by using 16 ns pulses as mw π/2-pulse and 12 μs as rf one.

2.4 *Calculation Details*

Calculations were performed with ORCA 3.0.3 program package [42]. **B3** geometry was optimized on UKS/B3LYP/cc-pVTZ level and is in good agreement with previously reported results. Hfc constants were calculated using density functional theory with B3LYP and PBE0 functionals and variety of full electron basis sets such as EPR-II [43], cc-pVTZ , aug-cc-pVTZ [44], N07D and N07T family (including diffuse functions) [45]. Fine Lebedev 770 angular grid and 10^{-10} Eh SCF convergence tolerance was used. Solvent effects were simulated with COSMO model [46].

3 Results and Discussion

3.1 *EPR spectroscopy*

Typical EPR spectrum of biradical **B3** at 298 K is shown in Fig. 3. The comparison of simulated and experimental spectra shows that they are in a very good agreement, and positions of all "exchange" lines in the magnetic field are practically coinside (Fig. 3). Similar EPR spectra were described in Refs. [25, 30].

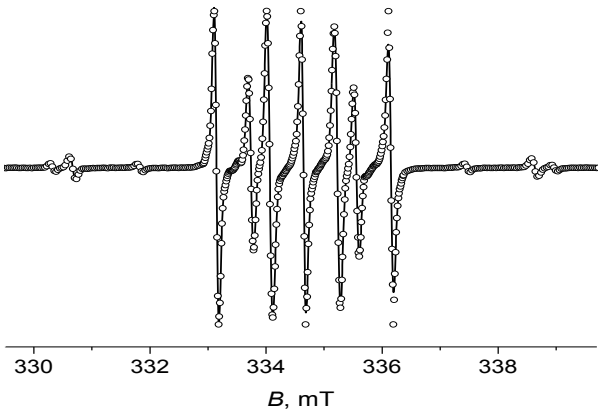

Fig. 3 Experimental (*solid line*) and calculated (*open circles*) EPR spectra of biradical **B3** in toluene at 298 K

Measured from spectra simulation value of the exchange integral $|J/a|$ at 298 K is equal to 3.4 ± 0.1 mT (a = 15.02 G), which is coincide with those published in Refs. [25, 30]. One can see from Fig. 3 that amplitudes of the central and high-field simulated main "radical" lines are bigger than

those of experimental ones. This is caused by the "stick" shape of the **B3** molecule, which is realized in the anisotropic rotation of **B3** performed in the experimental spectrum, while spectrum simulation has been done for the case of the isotropic rotation [39]. Positions of all the lines for both spectra are coinside.

Temperature dependences both of a and $|J/a|$ values for **B3** dissolved in toluene slightly decrease with the increase of temperature and coincide in the error limits with those reported in [30]: $\Delta H = -0.5 \pm 0.2$ kJ·mol^{-1} and $\Delta S = 6.8 \pm 0.7$ J·mol^{-1}·K^{-1}. Such small values were already explained in Ref. [30]: the barrier of rotation, E_a, of piperidine rings in biradicals with acetylene groups in the bridge is rather low as results from the DFT calculations: it does not exceed 8.0 kJ·mol^{-1} for **B3**. Librations of the piperidine planes relatively the p-C_6H_4 plane by up to 5 degrees have a value of E_a less than 0.1 kJ mol^{-1}, i.e., negligible. These results correlate well with the experimentally measured values of ΔH, which are equal to –0.5 kJ mol^{-1} and close to –1.0 kJ mol^{-1} in the case of **B3** dissolved in toluene and ethanol respectively. It should be also mentioned that such small values of E_a for biradical **B3** results in rather free intramolecular rotation of the nitroxide rings even at low temperatures, i.e., the EPR spectra and measured values of $|J/a|$ characterize not individual conformations of **B3** but an averaged pattern with very fast transitions between several rotamers, and the measured value of $|J/a|$ is averaged by all these conformations.

3.2 *ENDOR Investigation*

ENDOR spectra of biradicals **B3** and **B3a** are shown in Fig. 4. Signals of both samples are observed in the area of 3 MHz and 5 MHz, and we suppose that they reflect the interaction of the unpaired electron with a nuclear spin of nitrogen ^{14}N. Besides these signals, in the ENDOR spectrum of **B3** enriched with ^{13}C, two additional lines are observed in the area of 3.5-4.5 MHz. Subtracting the spectrum of the usual biradical **B3a** from the spectrum of **B3** results in the signal (Fig. 4 *c*), which contains only two peaks with a center at 3.7 MHz, what corresponds to a Larmor frequency of the carbon nucleus precession in the magnetic field, close to ~340 mT. The splitting between peaks is equal to 0.48 ± 0.14 MHz. These results clearly indicate that we observe a rather weak interaction between the unpaired electron and the ^{13}C carbon atom. The hfs constant value in such case is equal to the splitting, i.e., to 0.48 MHz. It should be noted that we could not determine all values of the anisotropic hfs tensor from our study of biradical **B3** in frozen toluene solutions.

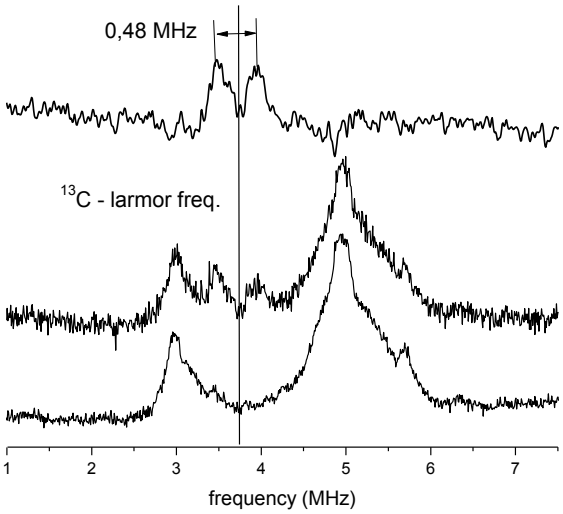

Fig. 4 ENDOR spectra of biradicals **B3a** (*a*) and **B3** (*b*). The spectrum (*c*) is a subtraction of (*a*) from (*b*). The estimated value of the hfs constant with ^{13}C is equal to ~0.48 MHz

3.3 *DFT calculations*

Important information about **B3** structure and features has been obtained from quantum chemical calculations. Calculated geometry of biradical **B3** is shown in Fig. 5, where the appropriate values of bond lengths, ^{13}C and other isotropic hfs constants on different atoms in **B3** are listed for two cases of calculation methods: B3LYP/N07D and PBE0/N07D. The whole set of ^{13}C isotropic hfs constant values calculated using B3LYP and PBE0 functionals at various basis sets is given in the Table. The distance between centers of N-O bounds is equal to 17.78 Å.

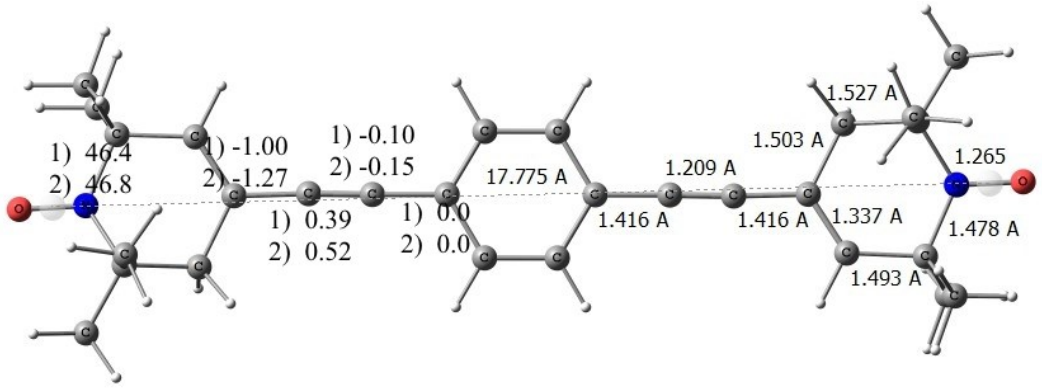

Fig. 5 Calculated bond lengths and ^{13}C isotropic hfs constants in biradical **B3**. Numbers *1*) and *2*) indicate the method of calculation of ^{13}C isotropic hfs constants: B3LYP/N07D and PBE0/N07D respectively

Table ^{13}C isotropic hfs constant values calculated using B3LYP and PBE0 functionals at various basis sets.

Method	$a(^{13}C)$, MHz
B3LYP/N07D	0.39
B3LYP/N07Ddiff	0.38
B3LYP/N07Tdiff	0.39
B3LYP/cc-pVTZ	0.33
B3LYP/aug-cc-pVTZ	0.35
B3LYP/EPR-II	0.38
PBE0/N07D	0.52
PBE0/cc-pVTZ	0.41
PBE0/aug-cc-pVTZ	0.43
PBE0/EPR-II	0.46
Experiment	0.48

It should be noted that calculations of the dipolar components of the hfs tensor can be systematically tuned by going to a much larger basis set of common use, isotropic hfc constants are usually reproduced better using a specialized basis set described in [45]. According to this note, we should point out two important results: firstly, specialized basis sets such as N07 family or EPR family, enable much better agreement with the experimental data than the conventional basis sets on a far less computational prices even in this case of very small hfs coupling. Secondly, we point out that for some reasons PBE0 functional systematically gives better agreement of calculated ^{13}C isotropic hfs constant with the experimental one in this particular case, while B3LYP functional in turn underestimates it, though both approaches yield results which are within the experimental error limits and agree well with the experimental value. We conclude that combination of PBE0/N07D or PBE0/EPR-II can be recommended to researchers as a cheap and precise way for computation of small hfs couplings in nitroxide biradicals.

4 Conclusion

A nitroxide biradical R_6–^{13}C≡C–*p*-C_6H_4–C≡^{13}C–R_6, **B3**, where R_6 = 1-oxyl-2,2,6,6-tetramethyl-3,4-ene- nitroxide ring, has been investugated by X-band EPR and electron-nuclear double resonance (ENDOR) spectroscopy. Spin density distribution and hyperfine splitting (hfs) constant value on ^{13}C atoms in the bridge in biradical **B3** were calculated using B3LYP and PBE0 functionals and several different basis sets including N07 family. These results were compared with the experimental value of the hfs constant on ^{13}C atoms measured from ENDOR

spectra of **B3**. A few recommendations concerning calculating of electron spin density distribution and the isotropic hfs constant values in nitroxide biradicals are given. Results presented in this paper confirm the fact that intramolecular electron spin exchange in **B3** biradical is realized by the indirect mechanism.

Acknowledgements This research was partly supported by Hungarian National, Research, Development and Innovation Office (OTKA104956). The study was also supported by the Supercomputing Center of M. V. Lomonosov Moscow State University [47]. AIK and OIG are thankful to Dr. E. N. Golubeva (Chemistry Department, M.V. Lomonosov Moscow State University) for helpful discussions, and to Dr. A. A. Shubin (G.K. Boreskov Institute of Catalysis, Siberian Branch of Russian Academy of Sciences) kindly provided us his program package.

References

1. M. Gomberg, J. Am. Chem. Soc. **22**, 757 (1900)

2. R.G. Hicks, (Ed.) *Stable Radicals: Fundamentals and Applied Aspects of Odd-Electron Compounds* (Wiley, West Sussex, 2010)

3. *Spin Labeling. Theory and Applications*, L.J. Berliner, ed., (Academic Press, New-York, London, 1976)

4. A.N. Kuznetsov, *The method of spin probes* (Nauka, Moscow, 1976)

5. G.I. Likhtenshtein, *Spin labeling methods in moleculat biology* (Wiley, New York, 1976)

6. A.M. Wasserman, A.L. Kovarsky, *Spin labels and probes in physical chemistry of polymers* (Nauka, Moscow, 1986)

7. *Imidazoline Nitroxides. Synthesis, Properties, Applications*, L.B. Volodarsky, ed., vol. 1, 2 (CRC Press, Boca Raton, FL, 1988)

8. S.S. Eaton, G.R. Eaton, *Measurements of interspin distances by EPR*. In: *Electron Paramagnetic Resonance* **19**, 318 (2004)

9. G. Likhtenshtein, J. Yamauchi, S. Nakatsuji, A.I. Smirnov, R. Tamura, *Nitroxides*: *Applications in Chemistry, Biomedicine, and Materials Science* (Wiley-VCH, New York, 2008)

10. K. Moebius, A. Savitsky, *High-field EPR spectroscopy on proteins and their model systems* (RSC Publishing, London, 2009)

11. H.P. Nguyen, A.M. Popova, K. Hideg, P.Z. Qin, BMC Biophysics **8**, 6 (2015)

12. C. Altenbach, C.J. López, K. Hideg, W.L. Hubbell, Methods Enzymol. **564**, 59 (2015)

13, S.M. Winter, S. Hill, R.T. Oakley, J. Am. Chem. Soc. **137**, 3720 (2015)

14. A. Rajca, Y. Wang, M. Boska, J.T. Paletta, A. Olankitwanit, M.A. Swanson, D.G. Mitchell, S.S. Eaton, G.R. Eaton, S. Rajca, J. Am. Chem. Soc. **134**, 15724 (2012)

15. T. Janoschka, N. Martin, U. Martin, C. Friebe, S. Morgenstern, H. Hiller, M.D. Hager, U.S. Schubert, Nature **527**, 78 (2015)

16. M. Rafiee, K.C. Miles, S.S. Stahl, J. Am. Chem. Soc. **137**, 14751 (2015)

17. M.Y. Zaremski, Polymer Sci., Ser. C **57**, 65 (2015)

18. F. Mentink-Vigier, U. Akbey, H. Oschkinat, S. Vega, A.J. Feintuch, Magn. Reson. **258**, 102 (2015)

19. C. Sauvée, M. Rosai, G. Casano, F. Aussennc, T.R. Weber, R. Ouari, P. Tordo, Angew. Chemie., Int. Ed. **52**, 10858 (2013)

20. A.I. Kokorin, V.N. Khrustalev, O.I. Gromov, Appl. Magn. Reson. **46**, 1429 (2015)

21. E.B. Böde, D. Margraf, J. Plackmeyer, G. Dürner, T.F. Prisner, O. Schiemann, J. Am. Chem. Soc. **129**, 6736 (2007)

22. E.G. Rozantsev, *Free Nitroxyl Radicals* (Plenum Press, New York, 1970)

23. A.B. Shapiro, M.G. Goldfield, E.G. Rozantsev, Tetrahedron Lett. **24**, 2183 (1973)

24. V.V. Pavlikov, A.B. Shapiro, E.G. Rozantsev, Izv. AN SSSR, Ser. Khim. No. 1, 128 (1980)

25. A.I. Kokorin, V.V. Pavlikov, A.B. Shapiro, Proc. Acad. Sci. USSR, Doklady Phys. Chem. **253**, 525 (1980)

26. S. Torii, T. Hase, M. Kuroboshi, C. Amatore, A. Jutand, H. Kawafuchi, Tetrahedron Lett. **38**(42), 7391 (1997)

27. A.I. Kokorin, Appl. Magn. Reson. **26**, 253 (2004)

28. A.I. Kokorin, V.A. Tran, K. Rasmussen, G. Grampp Appl. Magn. Reson. **30**, 35 (2006)

29. V.A. Tran, A.I. Kokorin, G. Grampp, and K. Rasmussen. Appl. Magn. Reson. **35**, 389 (2009)

30. A.I. Kokorin, E.N. Golubeva, B.Y. Mladenova, V.A. Tran, T. Ka´lai, K. Hideg, G. Grampp, Appl. Magn. Reson. **44**, 1041 (2013)

31. O.I. Gromov, E.N. Golubeva, V.N. Khrustalev, T. Ka´lai, K. Hideg, A.I. Kokorin, Appl. Magn. Reson. **45**, 981 (2014)

32. V.N. Parmon, A.I. Kokorin, G.M. Zhidomirov, *Stable Biradicals* (Nauka, Moscow, 1980)

33. V.N. Parmon, G.M. Zhidomirov, Mol. Phys. **27**, 367 (1974)

34. S.H. Glarum, J.H. Marshall, J. Chem. Phys. **47**, 1374 (1967)

35. H. Lemaire, J. Chim. Phys. **64**, 559 (1967)

36. T. Kálai, J. Jekő, Z. Berente, K. Hideg, Synthesis, 439 (2006)

37. J.A. Riddick, W.B. Bunger, K.T. Sakano, in: *Techniques of Chemistry*. Vol. II: *Organic Solvents, Physical Chemistry and Methods of Purification* (Wiley, New York, 1986)

38. Yu.N. Molin, K.M. Salikhov, K.I. Zamaraev, *Spin Exchange* (Springer, Berlin, 1980)

39. A.I. Kokorin, V.N. Parmon, A.A. Shubin, *Atlas of Anisotropic EPR Spectra of Nitroxide Biradicals* (Nauka, Moscow, 1984)

40. Ya.S. Lebedev, O.Ya. Grinberg, A.A. Dubinsky, O.G. Poluektov, in: *Bioactive spin labels*, ed. by R.I. Zhdanov (Springer, Berlin, 1992), pp. 228−254

41. W.B. Mims, Proc. Royal Soc. London **283**, 452 (1965).

42. F. Neese, *The ORCA program system* (Wiley Interdiscip. Rev., Comput. Mol. Sci. **2**, 73, 2012)

43. V. Barone, in: *Recent Advances in Density Functional Methods*, Part I, Ed. D.P. Chong (World Sci. Publ. Co., Singapore, 1996)

44. T.H. Dunning, Jr., J. Chem. Phys. **90**, 1007 (1989)

45. V. Barone, P. Cimino, E. Stendardo, J. Chem. Theory & Computation **4**, 751 (2008)

46. S. Sinnecker, A. Rajendran, A. Klamt, M. Diedenhofen, F. Neese, J. Phys. Chem. A **110**, 2235 (2006)

47. V. Sadovnichy, A. Tikhonravov, Vl. Voevodin, V. Opanasenko "Lomonosov, *Supercomputing at Moscow State University*, in: *Contemporary High Performance Computing: From Petascale toward Exascale*, pp. 283-307 (Chapman & Hall/CRC Computational Science, CRC Press, Boca Raton, USA, 2013)

Captions to Figures

Fig. 1 Scheme of the synthesis of biradical **B3**

Fig. 2 The scheme of the pulsed ENDOR experiment

Fig. 3 Experimental (*solid line*) and calculated (*open circles*) EPR spectra of biradical **B3** in toluene at 298 K

Fig. 4 ENDOR spectra of biradicals **B3a** (*a*) and **B3** (*b*). The spectrum (*c*) is a subtraction of (*a*) from (*b*). The estimated value of the hfs constant with ^{13}C is equal to ~0.48 MHz

Fig. 5 Calculated bond lengths and ^{13}C isotropic hfs constants in biradical **B3**. Numbers *1*) and *2*) indicate the method of calculation of ^{13}C isotropic hfs constants: B3LYP/N07D and PBE0/N07D respectively